AFRL-ML-WP-TP-2007-468

THERMALLY INDUCED STRESS INTENSITY IN A HOMOGENEOUS PLATE CONTAINING A FINITE LENGTH CRACK (PREPRINT)

George Jefferson

MAY 2007

Approved for public release; distribution unlimited.

STINFO COPY

This work was funded in whole or in part by Department of the Air Force contract FA8650-04-D-5233. The U.S. Government has for itself and others acting on its behalf an unlimited, paid-up, nonexclusive, irrevocable worldwide license to use, modify, reproduce, release, perform, display, or disclose the work by or on behalf of the U.S. Government.

MATERIALS AND MANUFACTURING DIRECTORATE
AIR FORCE RESEARCH LABORATORY
AIR FORCE MATERIEL COMMAND
WRIGHT-PATTERSON AIR FORCE BASE, OH 45433-7750

REPORT DOCUMENTATION PAGE

Form Approved
OMB No. 0704-0188

1. REPORT DATE *(DD-MM-YY)*	2. REPORT TYPE	3. DATES COVERED *(From - To)*
May 2007	Journal Article Preprint	

4. TITLE AND SUBTITLE
THERMALLY INDUCED STRESS INTENSITY IN A HOMOGENEOUS PLATE CONTAINING A FINITE LENGTH CRACK (PREPRINT)

5a. CONTRACT NUMBER
FA8650-04-D-5233

5b. GRANT NUMBER

5c. PROGRAM ELEMENT NUMBER
62102F

6. AUTHOR(S)
George Jefferson

5d. PROJECT NUMBER
2311

5e. TASK NUMBER
00

5f. WORK UNIT NUMBER
02

7. PERFORMING ORGANIZATION NAME(S) AND ADDRESS(ES)
UES Inc.
4401 Dayton-Xenia Road
Dayton, OH 45432-1894

8. PERFORMING ORGANIZATION REPORT NUMBER

9. SPONSORING/MONITORING AGENCY NAME(S) AND ADDRESS(ES)
Materials and Manufacturing Directorate
Air Force Research Laboratory
Air Force Materiel Command
Wright-Patterson AFB, OH 45433-7750

10. SPONSORING/MONITORING AGENCY ACRONYM(S)
AFRL-ML-WP

11. SPONSORING/MONITORING AGENCY REPORT NUMBER(S)
AFRL-ML-WP-TP-2007-468

12. DISTRIBUTION/AVAILABILITY STATEMENT
Approved for public release; distribution unlimited.

13. SUPPLEMENTARY NOTES
Journal article submitted to the ASME Journal of Engineering Materials and Technology. This work was funded in whole or in part by Department of the Air Force contract FA8650-04-D-5233. The U.S. Government has for itself and others acting on its behalf an unlimited, paid-up, nonexclusive, irrevocable worldwide license to use, modify, reproduce, release, perform, display, or disclose the work by or on behalf of the U.S. Government.

PAO Case Number: AFRL/WS 07-1031, 25 Apr 2007. Paper contains color content.

14. ABSTRACT
The delamination of orthotropic laminates containing finite-length cracks and subject to thermal gradients is examined. The exact limiting case solutions for infinitesimal- and infinite-length cracks are known, and are equal to each other when the crack length is approximately equal to the plate thickness. However, in the transition region of crack length from about 1 to 5 times the plate thickness, both limit solutions overestimate the energy release by 20-100%. Hence, an analysis was developed to better predict the energy release rate for such finite-length cracks. The model is a modification of the infinite-crack analysis of Hutchinson and Lu (1995, ASME J. Eng. Mat. Tech., 117 (4) pp. 386-390) and provides a closed form expression for the elastic energy release rate in a plane-strain orthotropic flat plate that agrees well with numerical values for cracks of length approximately half of the plate thickness and larger. The analytic result is shown to agree well with finite element results over a wide range of crack lengths, depths and interface conductivity, both for isotropic and orthotropic materials.

15. SUBJECT TERMS
Homogeneous Plate, Finite, Orthotropic Laminates

16. SECURITY CLASSIFICATION OF:			17. LIMITATION OF ABSTRACT:	18. NUMBER OF PAGES	19a. NAME OF RESPONSIBLE PERSON (Monitor)
a. REPORT	b. ABSTRACT	c. THIS PAGE			Randall S. Hay
Unclassified	Unclassified	Unclassified	SAR	20	19b. TELEPHONE NUMBER *(Include Area Code)* N/A

Standard Form 298 (Rev. 8-98)
Prescribed by ANSI Std. Z39-18

Thermally Induced Stress Intensity in a Homogeneous Plate Containing a Finite Length Crack

George Jefferson
Air Force Research Laboratory, Materials and Manufacturing Directorate
Wright Patterson Air Force Base, Ohio, USA, 45433
UES, Inc., Dayton OH 45432

The delamination of orthotropic laminates containing finite-length cracks and subject to thermal gradients is examined. The exact limiting case solutions for infinitesimal- and infinite-length cracks are known, and are equal to each other when the crack length is approximately equal to the plate thickness. However, in the transition region of crack length from about 1 to 5 times the plate thickness, both limit solutions overestimate the energy release by 20-100%. Hence, an analysis was developed to better predict the energy release rate for such finite-length cracks. The model is a modification of the infinite-crack analysis of Hutchinson and Lu (1995, *ASME J. Eng. Mat. Tech.*, **117** (4) pp. 386-390) and provides a closed form expression for the elastic energy release rate in a plane-strain orthotropic flat plate that agrees well with numerical values for cracks of length approximately half of the plate thickness and larger. The analytic result is shown to agree well with finite element results over a wide range of crack lengths, depths and interface conductivity, both for isotropic and orthotropic materials.

Introduction

Advanced high temperature materials such as ceramic composites are under active investigation for use in hot shell structures such as combustion liners. These materials are typically characterized by low thermal conductivity and a laminar structure with relatively low interlaminar strength. Consequently, the hot structures will be subject to large thermal gradients and thermal stress induced delamination initiated at internal interlaminar flaws are of significant concern. The thermal delamination problem has been studied extensively in the literature. The stress concentration due to an infinitesimal crack in an elastic body subject to a thermal gradient is given by Sih [1]. The complementary asymptotic linear elastic fracture solution for an infinitely long crack in an isotropic flat plate is given by Hutchinson and Lu [2] (H-L). These basic solutions are followed in the literature by analysis of more complex systems. Sorensen, Sarraute, Jorgensen and Horsewell [3] analyzed the long-crack problem for a laminate with dissimilar elastic laminae, and show that the interfacial energy release rate may be mitigated by selective layering of materials. Gu and Asaro [4] considered delamination fracture in continuously graded materials. The elastic-plastic problem was considered by Aoki, S., Kishimoto, K., and Sakata [5].

The present work focuses on the homogeneous orthotropic plate problem. Numerical investigation reveals that, with increasing crack length, the transition from the Sih infinitesimal crack result to the H-L infinitely long crack, or steady-state, solution is less abrupt than estimated by Hutchinson and Lu.

Here, we present a modification to the H-L result that provides a substantial improvement for finite length cracks (i.e. on the order of the plate thickness), while retaining the exact limiting result for arbitrarily long cracks.

The numerical work that motivated the present analysis was a straightforward 2-d plane strain ABAQUS[1] finite element model of a central crack in a flat plate subject to a prescribed temperature differential between the surfaces as shown in Figure 1. A focused mesh with second order quarter point elements at the crack tip, and reduced integration elements throughout was employed[6]. Energy release rates were calculated using the thermoelastic J-integral formulation built into the commercial code [7,8]. For verification, the calculated energy release rates were compared with the exact long-crack H-L solution and were found to be 25% below the asymptotic prediction for cracks as long as 3 times the plate thickness, with convergence to the asymptotic result confirmed only by modeling cracks 20-30 times the plate thickness. Thus it seemed appropriate to develop an analytic model to better predict the fracture behavior for such intermediate length cracks.

The H-L model is based on a long-crack isothermal fracture model of Hutchinson and Suo [9] along with several infinite crack approximations for the temperature distribution and resulting deformation due to a thermal gradient. Numerical simulation of the *isothermal* model shows that it performs remarkably well for cracks as short as twice the plate thickness. There are two key asymptotic kinematic assumptions in the thermoelastic analysis. 1) It is assumed that the upper and lower sections of the plate should have equal curvatures. 2) The in-plane strain parallel to the crack faces at the crack center is assumed to be equal on the opposed crack faces. By inspection of the numerical simulation, the equal curvature assumption proves to be quite good for relatively short cracks. The equal strain condition is, however, approached rather slowly with increasing crack length, and here an improvement is suggested.

Basic analysis summary

The essential calculation is the same here as in H-L, and so here we will highlight the key points as briefly as possible. The thermal load results in a set of resultant forces, P, and moments M_1, M_2 per unit out-of-plane thickness at the center of the crack as shown in Figure 2. The stress intensity is then calculated in terms of those end loads using the isothermal fracture formulation set forth in [9]. Referring to Figure 2, equilibrium requires $M_1 + M_2 = PH/2$. For a long crack the upper and lower plate sections are modeled as beams and the curvatures are asserted to be equal far from the crack tip, leading to the condition $M_1/H_1^3 = M_2/H_2^3$, thus

[1] Abaqus, Inc., Pawtucket R.I.

$$M_1 = \frac{\eta^3 PH}{2\left(1+\eta^3\right)} \ , \ M_2 = \frac{PH}{2\left(1+\eta^3\right)} \qquad (1)$$

where $\eta = H_1/H_2$. The analysis is restricted to $0 < \eta \le 1$, ie. if the crack is off center it must be nearer to the hot side of the plate to ensure an open mode crack [2]. Equation (1) is as-given in [2], however here we retain the resultant force *P* as an unknown.

The orthotropic thermo-elastic constitutive relation is of the form,

$$\begin{aligned} \varepsilon_{xx} &= \sigma_{xx}/E_x - \nu_{yx}\sigma_{yy}/E_y - \nu_{zx}\sigma_{zz}/E_z + \alpha_x \Delta T \\ \varepsilon_{xz} &= \sigma_{xz}/2\mu_{xz} \end{aligned} \qquad (2)$$

where $\varepsilon_{ij}, \sigma_{ij}$ are the components of strain and stress and expressions for the remaining strain components are obtained by suitable change of subscripts. E_i, μ_{ij}, ν_{ij} are the orthotropic elastic constants which satisfy the symmetry requirement, $\nu_{ij}E_j = \nu_{ji}E_i$, α_i are orthotropic thermal expansion coefficients and ΔT is a change in temperature.

Using Eq. (1), and assuming plane strain $\left(\varepsilon_{yy} = \varepsilon_{yz} = \varepsilon_{yx} = 0\right)$ the stress intensity factors are found directly using the analysis given in [9]. In the centered crack $\left(\eta = 1\right)$ case the crack tip field is pure mode II, with stress intensity factor,

$$K_{II}^{\eta=1} = \left(\frac{8}{\Lambda H}\right)^{1/2} P \qquad (3)$$

where

$$\Lambda \equiv \left(\frac{1+\rho}{2\lambda^{1/2}}\right)^{1/2} \qquad (4)$$

λ and ρ are the orthotropic material constants defined in[9] and in Lu, Xia and Hutchinson [10],

$$\lambda = \overline{E}_z/\overline{E} \qquad (5)$$

$$\rho = \lambda^{1/2}\left(\frac{\overline{E}}{2\mu_{xz}} - \frac{\nu_{xz}+\nu_{xy}\nu_{yz}}{1-\nu_{xy}\nu_{yx}}\right) \qquad (6)$$

where $\overline{E} \equiv E_x/\left(1-\nu_{xy}\nu_{yx}\right)$ and $\overline{E}_z \equiv E_z/\left(1-\nu_{zy}\nu_{yz}\right)$ are the effective plane strain moduli for in-plane uniaxial stressing in each of the principle directions. See also Krenk [11], using $\rho = \kappa$ and $\lambda = \delta^{-4}$. Note that $\lambda, \rho,$ and Λ are all unity for an isotropic material.

In the general case for $0 < \eta \le 1$ the crack is mixed mode with the energy release rate and stress intensity factors,

$$
\begin{aligned}
G &= \frac{\Lambda}{\bar{E}}\left(\left(K_I/\lambda^{1/4}\right)^2 + K_{II}^2\right) = \frac{P^2(1+\eta)^5}{2\bar{E}H\eta\left(1+\eta^3\right)} \\
K_{II} &= K_{II}^{\eta=1}\Gamma \\
K_I &= \lambda^{1/4}\left(G\bar{E}/\Lambda - K_{II}^2\right)^{1/2}
\end{aligned}
\qquad (7)
$$

Where Γ is the ratio of mode II stress intensity to the $\eta = 1$ stress intensity,

$$
\Gamma = \left(\frac{1+\eta}{2\eta}\right)^{1/2}\left\{\frac{\sin\omega}{2\sqrt{2U}} + \frac{(\eta+1)\eta^2}{4\left(1+\eta^3\right)}\frac{\cos\omega+\gamma}{\sqrt{2V}}\right\} \qquad (7a)
$$

and U, V, w, γ are the dimensionless functions of η,

$$
\begin{aligned}
1/U &= (1+\eta)(1+3\eta(1+\eta)) \\
1/V &= 12\left(1+\eta^3\right) \\
\sin\gamma &= 6\eta^2(1+\eta)\sqrt{UV} \\
\omega &\cong 3°(1-\eta) + \sin^{-1} 2/\sqrt{7}
\end{aligned}
\qquad (8)
$$

Kinematic constraint

In place of the H-L condition of strain equality at the crack center, the kinematic condition we will impose is that the deformed lengths of the upper and lower crack faces must be equal. This leads to the condition,

$$
\int_0^a \left(\varepsilon_{xx}^{(+)} - \varepsilon_{xx}^{(-)}\right) dr = 0 \qquad (9)
$$

where ε_{xx} is the strain parallel to the crack face, *r* is the coordinate along the crack measured from the tip, and superscripts (+) and (-) denote the upper and lower faces respectively. The orthotropic plane strain constitutive relation on the traction-free faces is,

$$
\varepsilon_{xx}^{(\pm)} = \frac{\sigma_{xx}^{(\pm)}}{\bar{E}} + \bar{\alpha}T^{(\pm)}, \qquad (10)
$$

where σ_{xx} is the stress parallel to the crack face. $\bar{\alpha} \equiv \alpha_x + \nu_{yx}\alpha_y$, is the plane strain thermal expansion coefficient, and *T* is the crack face temperature The $(\pm)$ notation is used to indicate that this is a pair of equations separately relating the quantities on each face. Combining Eq. (9) and Eq. (10) yields,

$$
\int_0^a \left(\sigma_{xx}^{(+)} - \sigma_{xx}^{(-)}\right) dr + \bar{E}\bar{\alpha}a\phi(T_1 - T_2) = 0 \qquad (11)
$$

where T_1, T_2 are the temperatures at the plate surfaces and we define the average temperature jump ϕ,

$$
\phi \equiv \frac{1}{T_1 - T_2}\frac{1}{a}\int_0^a \left(T^{(+)} - T^{(-)}\right) dr \qquad (12)
$$

For comparison with the H-L formulation, for a sufficiently long crack, far from the crack tip, the heat conduction through the plate is 1D and the jump in face temperatures away from the crack tip will be determined by the conduction across the crack as,

$$\left.\frac{T^{(+)}-T^{(-)}}{T_1-T_2}\right|_{x=0}=\frac{1}{1+B_c} \qquad (13)$$

where the Biot number, B_c, characterizes the heat flow across the open crack, with $B_c=0$ for a perfectly insulating crack, and $B_c\to\infty$ for perfect conduction[2]. Near to the tip, heat flux around the tip reduces the temperature jump across the faces. However in the limit $a>>H$ the influence of the crack tip field becomes vanishingly small, so that $\phi\to\left(1+B_c\right)^{-1}$. For any finite length crack $0<\phi<\left(1+B_c\right)^{-1}$.

By inspection of numerical results, for cracks that are approximately equal to the plate thickness and larger, the stress along the crack faces is well approximated by matching the asymptotic crack tip (Paris and Sih, [12]) and far-field (beam theory) solutions,

$$\sigma_{xx}^{(\pm)}=\begin{cases}\sigma_0^{(\pm)} & r^{*(\pm)}\le r\le a\\ -s^{(\pm)}K_{II}\Lambda\left(\dfrac{2}{\pi\, r}\right)^{1/2} & 0\le r\le r^{*(\pm)}\end{cases} \qquad (14)$$

where $\sigma_0^{(\pm)}$ is the value of the tangential stress at the plate center, and the sign indicator $s^{(+)}\equiv 1; s^{(-)}\equiv -1$, is introduced because the stress is compressive on the upper face and tensile on the lower. The transition radius, $r^{*(\pm)}$ is the distance from the crack tip (generally different on each face) where the two limiting forms are equal, which is simply,

$$r^{*(\pm)}=\frac{2}{\pi}\left(\frac{\Lambda K_{II}}{\sigma_0^{(\pm)}}\right)^2 \qquad (15)$$

Figure 3 shows the piecewise stress approximation compared with numerical results. It should be noted that the piece-wise function is somewhat lower than the actual distribution near $r^{*(\pm)}$, which ultimately results in an over (i.e. conservative) estimate of the energy release rate. The crack face stress far from the crack tip, $\sigma_0^{(\pm)}$, is found directly from beam theory (as in H-L),

$$\sigma_0^{(\pm)}=-s^{(\pm)}\frac{8P}{H}g^{(\pm)}(\eta) \qquad (16)$$

where,

$$g^{(\pm)}(\eta)=\frac{(1+\eta)^5}{16\eta(1+\eta^3)}\left(1+s^{(\pm)}\frac{(1-\eta)(1-4\eta+\eta^2)}{(1+\eta)^3}\right) \qquad (17)$$

so that,

$$r^{*(\pm)} = \frac{\Lambda H}{4\pi}\left(\frac{\Gamma}{g^{(\pm)}}\right)^2 \qquad (18)$$

recalling that Γ is the stress intensity ratio given by Eq (7a). Clearly the present analysis must be restricted to cases where $a > r^{*(\pm)}$. However as $r^{*(\pm)}$ represents the size of the crack tip dominated region we will conservatively also restrict application to $H_1 > 2r^{*(\pm)}$, which is ensured for the isotropic case if $0.2 \le \eta \le 1$. The maximum value of $r^{*(\pm)}$ *in that range* is $\sim H/10$ at $\eta \cong 0.5$.

The crack length condition, Eq. (11), can now be integrated and solved for *P*,

$$P = \frac{\eta\left(1+\eta^3\right)\bar{E}\,\bar{\alpha}H\phi\left(T_1 - T_2\right)}{\left(1+\eta\right)^5\left[1+\frac{H\Lambda}{4\pi a}\frac{\Gamma^2}{g^{(+)}g^{(-)}}\right]} \qquad (19)$$

In the large *a* limit, and using $\phi = \left(1+B_c\right)^{-1}$, we recover the H-L result exactly,

$$P = \frac{\eta\left(1+\eta^3\right)\bar{E}\,\bar{\alpha}H\left(T_1 - T_2\right)}{\left(1+\eta\right)^5\left(1+B_c\right)} \qquad (20)$$

Finally, the stress intensity and energy release rate are found by substituting Eq (19) into Eq (7), e.g.

$$\frac{G}{\bar{E}H\left[\bar{\alpha}\left(T_1 - T_2\right)\right]^2} = \frac{\eta\left(1+\eta^3\right)\phi^2}{\left(1+\eta\right)^5 2\left[1+\frac{H\Lambda}{4\pi a}\frac{\Gamma^2}{g^{(+)}g^{(-)}}\right]^2} \qquad (21)$$

It is notable that the quantity $\Gamma^2/g^{(+)}g^{(-)}$ is approximately 1 for $0.5 \le \eta \le 1$. The large *a* limit of (19) of course agrees with H-L, hence we will use the $a \to \infty, \eta = 1$, perfectly insulating $\left(\phi \to 1\right)$, case as a baseline for comparison of solutions,

$$G_{HL} = \bar{E}H\left[\bar{\alpha}\left(T_1 - T_2\right)\right]^2/32 \qquad (22)$$

For reference the small-crack isotropic limit of Sih [1] is,

$$G_0 = 2\pi G_{HL}\left(\frac{a}{H}\right)^3 \qquad (23)$$

Temperature distribution

As will be shown, Eq (19) represents an improvement over Eq (20) even if the crack face temperature distribution is approximated by taking $\phi = \left(1+B_c\right)^{-1}$. However, further improvement is realized by calculating ϕ from Eq. (12) using the true temperature distribution. Unfortunately, although the asymptotic temperature distributions near the tip and far field are known (Florence and Goodier, [13]), assuming a piecewise temperature distribution similar to Eq. (14) does not prove sufficiently accurate. Therefore we will rely on numerically generated results to derive an functional dependence of ϕ on the plate geometry. The thermal finite element analysis was performed using a thermal

contact relation over the crack surface such that the heat flux across the crack is $q = B_c k \left(T^{(+)} - T^{(-)}\right)/H$, where k is the (isotropic) thermal conductivity of the plate. Note that the heat transfer across a physical crack is, in general, strongly dependant on the crack opening, however here we have assumed that local variation of the crack opening over the crack length may be neglected and that B_c is an effective value which accounts for the average crack opening. The consequences of this assumption will be discussed in a subsequent section.

A high quality general fit to the numerical results is found by arguing as follows. For sufficiently long cracks, increasing the crack length does not significantly affect the non-uniform field near the tip, further, for an infinite crack we require $\phi = (1+B_c)^{-1}$, therefore we fit our numerical simulation results to the form,

$$\phi = \frac{1}{1+B_c}\left(1 - C\frac{H}{a}\right) \qquad (24)$$

where C is a function of B_c and η. C is determined from numerical solution of the heat transfer problem as the large a limit of the quantity $(1-(1+B_c)\phi)(a/H)$, which converges to a constant quickly with increasing crack length ($(a/H) = 2-3$ is sufficient). We find that for cracks longer than $a \cong H$,

$$\phi = \frac{1}{1+B_c}\left(1 - \frac{\xi(\eta)}{(1+B_c)^{2/3}}\frac{H}{a}\right) \qquad (25)$$

where the dependence on B_c is empirical. The value of ξ is only weakly dependant on η over the range $0.5 < \eta < 1$, having values of $\xi \cong 0.2112$ at $\eta = 1$ and $\xi \cong 0.2288$ at $\eta = 1/2$. As Figure 4 shows, this is an excellent fit to numerically derived values for all B_c and for $2a > H$. Equation (25) is clearly not valid for $a/H \le \xi(1+B_c)^{-2/3}$, but this restriction is in line with other aspects of the analysis.

Results and Discussion

Figure 5 shows the energy release rate calculated using Eq (21), with ϕ from Eq (25) as well as the approximation, $\phi = (1+B_c)^{-1}$, for comparison. The full calculation shows good (and as expected slightly conservative) agreement with the finite element results. Ignoring the near-tip temperature variation results in a substantially higher energy release rate prediction, although it still provides some improvement over the asymptotic result.

Figure 6 shows the effectiveness of the analysis for variation of both η and B_c. The agreement with numerical results is best for η=1 and somewhat decreases, becoming more conservative, for off-center cracks. As noted previously this analysis is not intended for significantly smaller values of η (as for example subsurface cracks), where the difference undoubtedly increases.

It is worthwhile to refer to Figure 6 in discussing the effect of the constant B_c assumption. The analysis shows a slightly increasing energy release rate for decreasing η at a fixed value of B_c. However, realistically, the heat transfer coefficient itself decreases substantially (potentially by orders of magnitude) as the crack opens and the mechanism of transfer transitions from contact conduction to gas transport and radiation (H-L). As η is decreased, the stress intensity becomes increasingly mode I, therefore the crack opens further. Consequently if the dependence of heat conduction on the crack opening is accounted for then the dependence of G on η may be far more pronounced than suggested by Figure 6. This aspect of the problem is discussed in detail in H-L and is not qualitatively affected by the present analysis.

Closure

In closing we note that although the examples given have been for isotropic materials the formulation holds quite well for orthotropic materials as well. Eq. (19) predicts that the energy release rate will be reduced for large values of the parameter Λ, while the H-L result is independent of any orthotropy (the orthotropy affects only the mode mixity). Large Λ corresponds to small values of through-thickness moduli, E_z and μ_{xz}, which is notably typical of many composite systems. As an example we consider in-plane isotropy, and fix $\nu_{xy} = \nu_{yx} = 0.1$, $\nu_{xz} = \nu_{yz} = 0.15$ and $\lambda = 1/2$. Figure 7. shows the theory along with finite element results for $\eta = 1$ and $\eta = 1/2$ as the in-plane shear modulus is varied. The model correctly predicts the reduction in release rate for low shear, however the effect is significant in this example only for very small values.

Acknowledgment

This work was performed while the author held a National Research Council Research Associateship Award at the Air Force Research Laboratory Materials and Manufacturing Directorate.

Nomenclature

a	crack half-length
H, H_1, H_2	total, upper, and lower thickness
η	thickness ratio
x,y,z	orthogonal coordinates
r	coordinate from tip along face
T	temperature.
T_1, T_2	temperatures, plate surfaces
$P,\ M_1, M_2$	resultant force and moments
$\varepsilon_{ij}, \sigma_{ij}$	components of strain and stress
E_i, μ_{ij}, ν_{ij}	elastic constants
α_i	thermal expansion coefficients
$\overline{E}, \overline{E}_z$	effective moduli
$\overline{\alpha}$	effective thermal expansion
K_I, K_{II}	stress intensity factors

$K_{II}^{\eta=1}$	stress intensity factor for $\eta=1$
G	energy release rate.
G_0, G_{HL}	asymptotic limits of G.
λ, ρ, Λ	orthotropic material constants
ϕ	average temperature jump
B_c	Biot number
σ_0	far field crack face stress
$s^{(\pm)}$	sign indicator
r^*	transition radius
k	thermal conductivity
q	heat flux
dimensionless functions of η	
U, V, w, γ	stress intensity decomposition
g	Eq (17), $g(\eta=1)=1$
Γ	ratio $K_{II}(\eta)/\ K_{II}^{\eta=1}$, $\Gamma(\eta=1)=1$
ξ	fit parameter
superscripts	
(+) (-)	upper and lower crack face
(±)	quantity in equation applied separately to each face.

References

[1] Sih, G.C., 1962, "On the Singular Character of Thermal Stresses Near a Crack Tip," *ASME Journal of Applied Mechanics* Vol 117 pp. 386-390.

[2] Hutchinson, J.W. and Lu, T.J. 1995, "Laminate Delamination Due to Thermal Gradients," *ASME Journal of Engineering Materials and Technology*, Vol 117 (4) pp. 386-390.

[3] Sorensen, B.F., Sarraute, S., Jorgensen, O. and Horsewell, A., 1998, "Thermally Induced Delamination of Multilayers," *Acta Materialia* Vol. 46 (8) pp. 2603-2615.

[4] Gu, P. and Asaro, R.J., 1997, "Cracks in Functionally Graded Materials," *International Journal of Solids and Structures*. Vol 34 (1) pp. 1-17.

[5] Aoki, S., Kishimoto, K., and Sakata, M., 1982, "Elastic-plastic Analysis of Crack in Thermally-loaded Structures," *Engineering Fracture Mechanics*, Vol 16 (3) pp. 405-413.

[6] Barsoum, R.S., 1976, "On the Use of Isoparametric Finite Elements in Linear Fracture Mechanics," *International Journal for Numerical Methods in Engineering*. Vol 10 (1) pp. 25-37.

[7] ABAQUS Theory Manual, Version 6.4, 2003, Section 2.16.1, ABAQUS, Inc, Pawtucket, RI.

[8] Kishimoto, K., Aoki, S. and Sakata, M. 1980, "On the Path Independent Integral-J," *Engineering Fracture Mechanics*, Vol 13 (4) pp. 841-850.

[9] Hutchinson, J.W. and Suo, Z. 1992, "Mixed Mode Cracking in Layered Materials," in *Advances in Applied Mechanics* Vol 29, edited by J. W. Hutchinson and T. Y. Wu. (Academic Press, Boston) pp. 63-191.

[10] Lu, T.J., Xia, Z.C., and Hutchinson, J.W. , 1994, "Delamination of Beams Under Transverse Shear and Bending," *Materials Science and Engineering A* 188 (1-2) pp. 103-112.

[11] Krenk, S., 1979,. "On the Elastic Constants of Plane Orthotropic Elasticity," *Journal of Composite Materials*. Vol 13 (2) pp. 108-116.

[12] Paris P. C. and Sih, G.C. 1965, "Stress Analysis of Cracks" in Fracture Toughness Testing and Its Applications, ASTM STP 381, American Society for Testing and Materials, Philadelphia.

[13] Florence, A.L. and Goodier, J.N., 1960, "Thermal Stresses Due to Disturbance of Uniform Heat Flow by an Insulated Ovaloid Hole," *ASME Journal of Applied Mechanics* Vol. 27 (4) pp. 635-639.

Figures

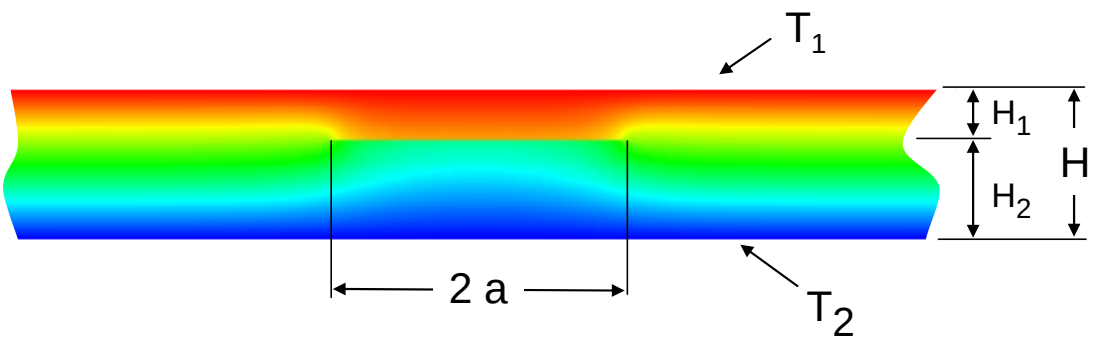

Figure 1. Geometry of an infinite flat plate with a finite length central crack. Configuration shown is $a = H$, $H_1/H_2 = 1/2$. Contour shading shows the numerically calculated temperature distribution for a partly conducting crack $(B_c = 1)$.

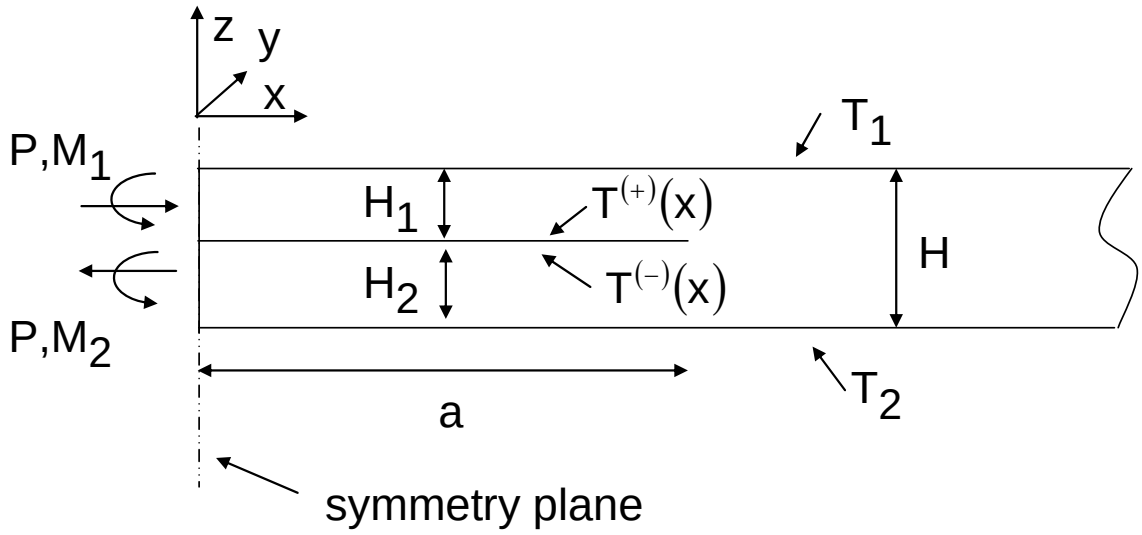

Figure 2. Plane geometry of a thermally loaded center cracked plate showing the resultant force and moments at the central symmetry plane. Surface temperatures T_1, T_2 are fixed with $T_1 > T_2$, while crack face temperatures $T^{(+)}, T^{(-)}$ are dependant on position along the crack face.

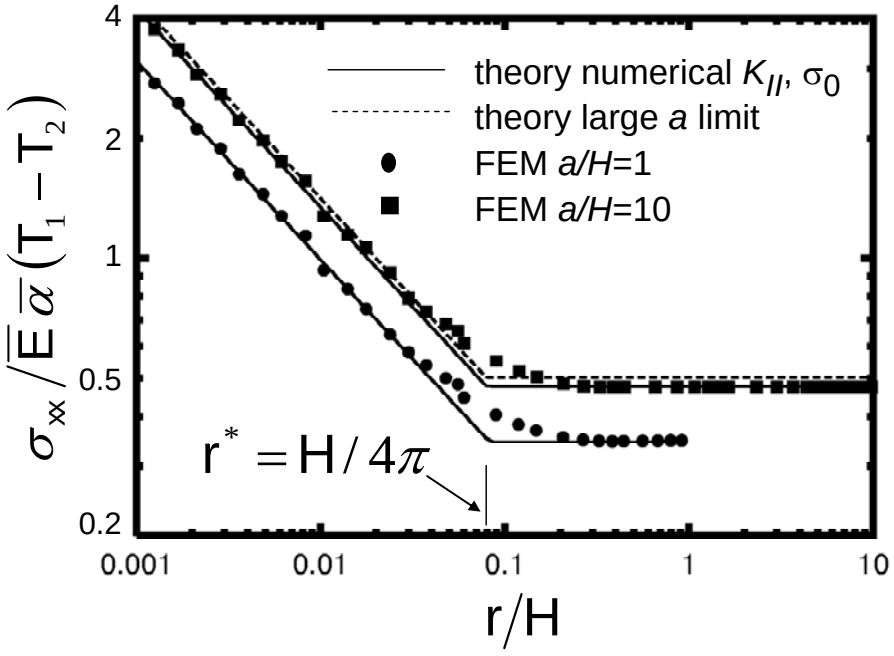

Figure 3. Piecewise stress distribution function. Examples shown are for $\eta = 1$, $\Lambda = 1$ and $B_c = 0$. For the symmetric case the absolute value of the stress (shown) is the same on upper and lower faces. The theory lines are calculated using Eq. (14) with K_{II} and σ_0 a) extracted from the finite element solution (solid lines) and b) based in the large *a* limit, $|\sigma_0| = \overline{E}\,\overline{\alpha}(T_1 - T_2)/2$, $K_{II} = \overline{E}\,\overline{\alpha}(T_1 - T_2)(2H)^{1/2}/8$ (dashed line).

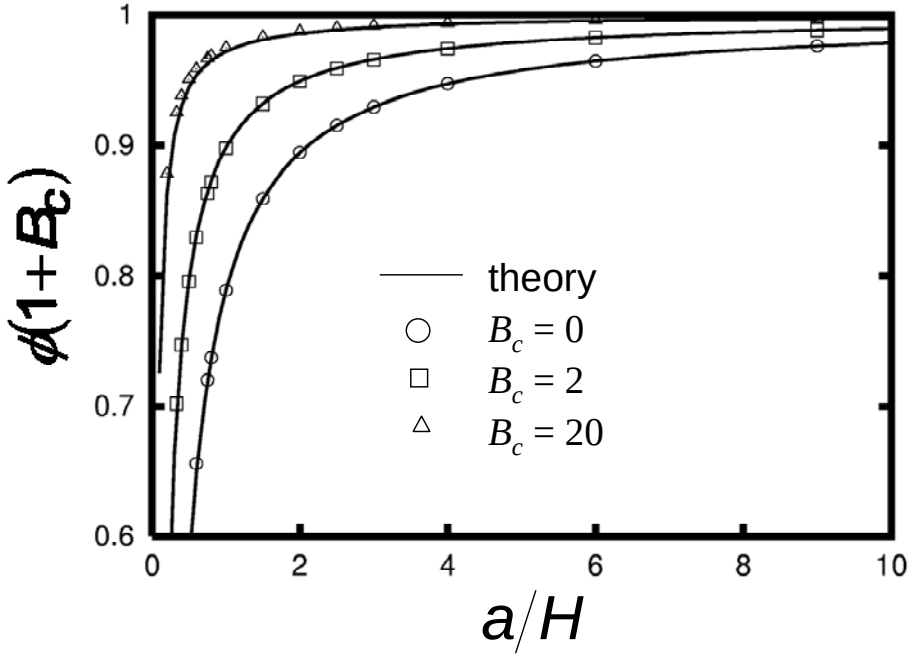

Figure 4. Average temperature jump across crack face for a centered crack $(\eta = 1)$. Markers are based on finite element results, calculated using Eq. (12). Theory lines are Eq. (25) with fit parameter $\xi = 0.2112$. The fit is remarkably good for a wide range of B_c and a/H.

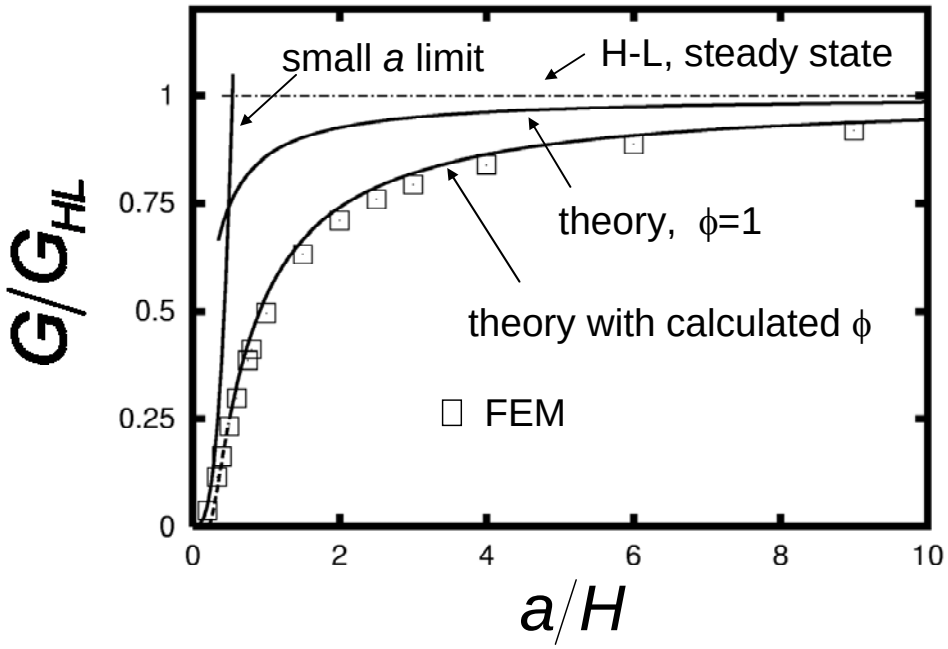

Figure 5. Energy release rate, for $\eta = 1$, $\Lambda = 1$ and $B_c = 0$. Theory lines are Eq. (21) using $\phi = 1$, for a fully analytic result that demonstrates an improvement over the infinite crack length solution. Using the improved value of ϕ from Eq. (25) yields an excellent fit to the numerical results. The calculation is remarkably well behaved for shorter cracks than one might expect (dashed region), it does however become non-conservative go to zero at nonzero *a* .

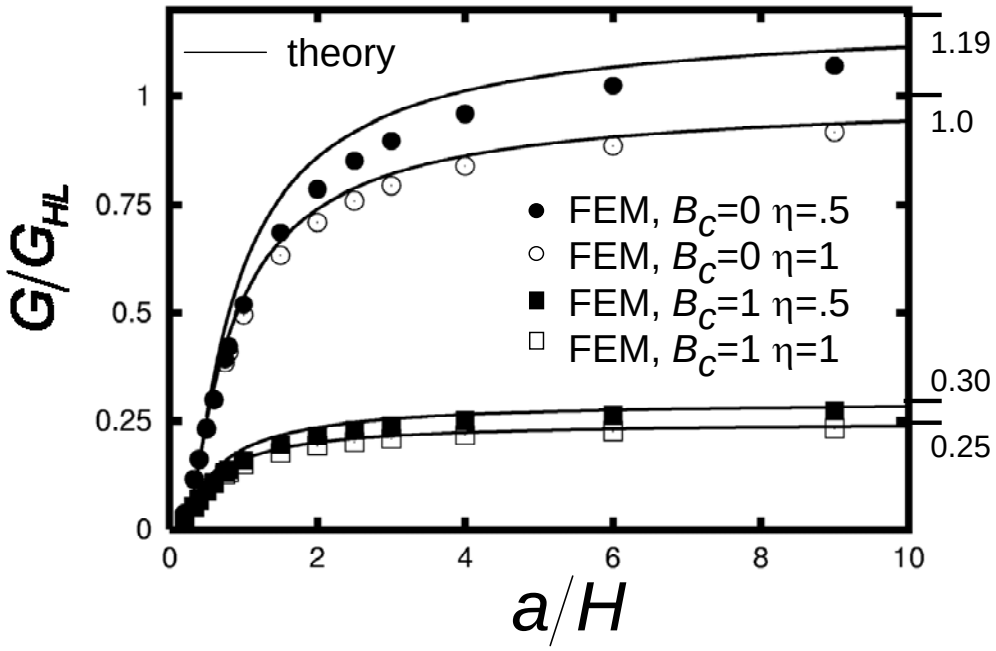

Figure 6. Energy release rate for the isotropic case $(\Lambda = 1)$, for $\eta = 1, 1/2$, and $B_c = 0, 1$. The theory, Eq's. (21) and (25), fits best for $\eta = 1$, and provides a conservative estimate for off-center cracks. The numeric values to the right are the exact asymptotic values for the four cases from Eqn's (7), and (20).

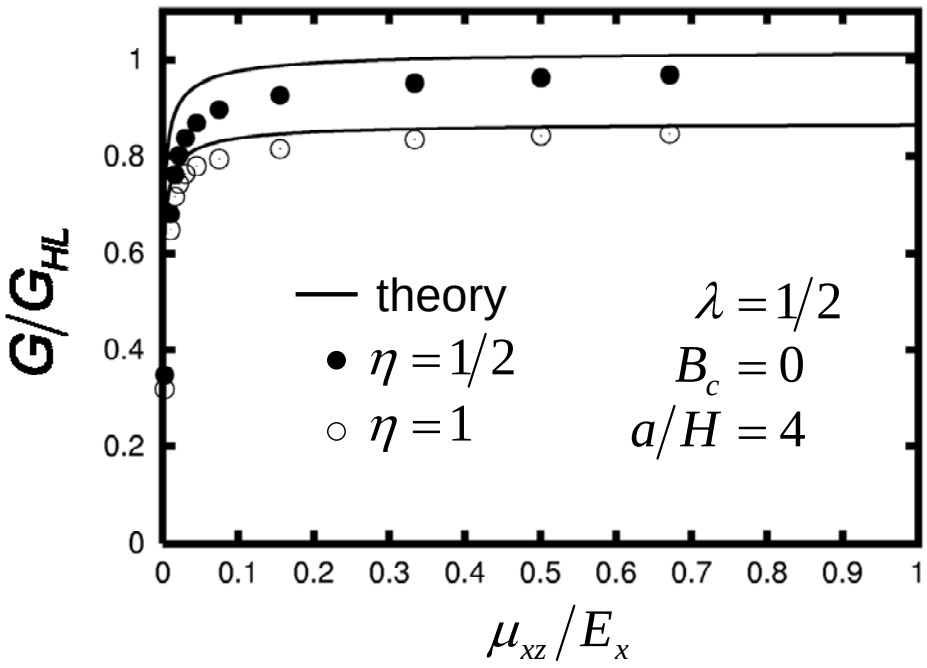

Figure 7. Orthotropic example. Normalized energy release rate for $a/H = 4, \lambda = 1/2, B_c = 0$ showing the variation with shear modulus. Reduced energy release rate is predicted by both theory and numerical simulation, but only for very small values of μ_{xz}.